couragement and for her permission to use the facilities of her department. Thanks are also due to the Department of Physics, Faculty of Science, Alexandria University, Alexandria, U.A.R., where most of the calculations were carried out.

References

AKAMATSU, N. & MATSUNAGA, Y. (1956). Bull. Chem. Soc. Japan, 29, 800.
BANERJEE, K. & BHATTACHARJYA, J. (1938). Science and Culture, 4, 60.
BANERJEE, S. (1938). Z. Kristallogr. A 100, 316.
BROWN, G. M., NORMENT, H. G., JR & LEVY, H. A. (1957). Acta Cryst. 10, 806.
CRUICKSHANK, D. W. J. (1956). Acta Cryst. 9, 915.
FRENCH, C. M. (1945). Trans. Faraday Soc. 41, 676.
GOODWIN, T. H., PRZYBYLSKA, M. & ROBERTSON, J. M. (1950). Acta Cryst. 3, 279.
GORDON, D. A. (1960). J. Phys. Chem. 64, 273.

HOARAU, J., JOUSSOT-DUBIEN, J., LEMANCEAU, B., LUMBROSO, N. & PACAULT, A. (1956). Cahier de Physique, no. 74, 34.
KRISHNAN, K.S. & BANERJEE, S. (1935). Phil. Trans. A 234, 265.
LASHEEN, M. A. (1964). Phil. Trans. A 256, 357.
LASHEEN, M. A. & KORAYEM, M. T. (1967). To be published.
LASHEEN, M. A. & TADROS, S. (1968). Acta Cryst. A 24, 287.
LONSDALE, K. & KRISHNAN, K. S. (1936). Proc. Roy. Soc. A 156, 597.
LUMBROSO-BADER, N. (1956). Ann. Chim. 13, 687.
MARSH, R. E. (1958). Acta Cryst. 11, 654.
MATHIESON, A. McL., ROBERTSON, J. M. & SINCLAIR, V. C. (1950). Acta Cryst. 3, 245.
PACAULT, A. (1946). Ann. Chim. 12, 527.
PERCEAU, R. (1953). C.r. Acad. Sci. Paris, 236, 76.
SAKURAI, T. (1962). Acta Cryst. 15, 1164.
SINCLAIR, V. C., ROBERTSON, J. M. & MATHIESON, A. McL. (1950). Acta Cryst. 3, 231.
SUTOR, D. J. (1958). Acta Cryst. 11, 83.
TROTTER, J. (1961). Acta Cryst. 14, 244.
TULINSKY, A. & WHITE, J. G. (1958). Acta Cryst. 11, 7.
WALLEY, D. (1967). Private communication.

Crystal Diffraction Profiles for Monochromatic Radiation*

BY J. A. BEARDEN, JOHN G. MARZOLF† AND JOHN S. THOMSEN

Department of Physics, The Johns Hopkins University, Baltimore, Maryland, U.S.A.

The instrumental window of a double crystal spectrometer in the dispersive (1, +1) position has been determined experimentally with a Mössbauer source and compared with theoretical predictions. The experiment was done at a wavelength of 0·86 Å* with the 14·4 keV γ ray that follows the $^{57}Co \rightarrow {}^{57}Fe$ decay. The crystals employed were quartz (10$\bar{1}$1), silicon (111), germanium (111), and calcite (211) (10$\bar{1}$4), where the indices refer to the structural cells. The theoretical expression for the double-crystal window was calculated as the convolution of the appropriate single-crystal monochromatic profiles predicted by the Darwin–Prins dynamical theory of X-ray diffraction. The agreement between theory and experiment was good and clearly shows the necessity for crystal asymmetry corrections to precision wavelength determinations in certain cases.

Introduction

Less than two years after von Laue had suggested the possibility of crystal diffraction of X-rays, Darwin (1914) published a pair of papers outlining the dynamics of the process. A number of years later this theory was expanded by Prins (1930) to include absorption effects; but, because of the difficulty in obtaining a monochromatic radiation source in the X-ray region, it has only recently become possible to test the theory adequately. Moreover, the theory predicts asymmetric diffraction profiles under certain conditions, and such profiles are of considerable importance in the

determination of X-ray wavelengths with the precision now required for studies such as the atomic constants evaluation.

Investigations with the two-crystal spectrometer permit certain aspects of the theory to be checked, such as the widths of the diffraction profiles in the non-dispersive spectrometer configurations (Parratt, 1932; Allison, 1932; Parratt & Miller, 1936). These experiments, however, give little information as to the shape of these patterns. In fact, for a pair of identical crystals they can yield no information at all about the asymmetry of either the single-crystal profiles or the double-crystal patterns in the dispersive positions of the spectrometer (the configurations required for wavelength determination).

The first step toward the solution of this problem came with DuMond's suggestion in 1937 for a multiple (3 or more) crystal spectrometer (DuMond, 1937; Boll-

man, Bailey & DuMond, 1938). This proposal recommended a non-dispersive configuration which did not yield conclusive results, but Renninger (1955) adapted the idea to the plus position of the spectrometer and observed a single-crystal profile from calcite with copper X-rays. Since then he and others (Renninger, 1960, 1967; Bubáková, Drahokoupil & Fingerland, 1960, 1961) have investigated silicon and germanium with this method, and have obtained moderately good agreement with the theory. A second approach emerged from Borrmann's (1941, 1950) experiments with the transmission of X-rays through thin single crystals. Brogren & Adell (1954) developed this technique, which employs a two-crystal spectrometer in the non-dispersive $(n, -n)$ position with the second crystal used in transmission. Theoretically such a crystal possesses a symmetric diffraction profile, and may thus be used as a probe to investigate any asymmetry in the first crystal.

The problem has been very recently attacked by still a third method (Kohra, 1962) that also employs a two-crystal spectrometer in the minus position. Here, one of the crystals is cut with the atomic planes inclined to the front face so that the reflected beam leaves the face at an angle which is small compared with the Bragg angle. Theoretically, this produces a narrower monochromatic profile, and hence may be used to study the other crystal.

The development in recent years of reasonably intense Mössbauer sources has provided a monochromatic radiation source, and the present investigation employed this technique. The 14·4 keV γ ray emitted by ^{57}Fe was used as the radiation source, and the crystals studied were quartz, silicon, germanium, and calcite.

Theoretical calculations

The geometrical corrections for the double-crystal spectrometer have been analyzed by Schwarzschild (1928); a comprehensive treatment of the instrument may be found in Compton & Allison (1935), including a derivation for the plus position monochromatic profile (i.e., the instrumental window). Their result (with all angles expressed in radians) is

$$P(\psi) = \int_{-\phi_m}^{\phi_m} \int_{-\infty}^{\infty} G(\theta - \theta_0, \varphi) I_1(\theta - \theta_0$$
$$- \tfrac{1}{2}\varphi^2 \tan \theta_0) I_2(\psi - \theta + \theta_0 - \tfrac{1}{2}\varphi^2 \tan \theta_0) d\theta d\varphi . \quad (1)$$

In this equation $G(\theta - \theta_0, \varphi)$ describes the incident intensity distribution (which is mainly determined by geometrical limitations due to slits, etc.) as a function of the horizontal angle θ (with θ_0 denoting the Bragg angle) and the vertical angle φ (measured about a hori-

zontal plane). ψ measures the angle between the first and second crystals, which are so aligned that the normals to the reflecting atomic planes of both crystals lie in a horizontal plane; $P(\psi)$ represents the observed intensity as a function of this angle. The vertical limiting slits are adjusted so that the incident beam is symmetrical about the horizontal, and φ_m is the maximum angle of vertical divergence.

I_1 and I_2 are the single-crystal profiles for the first and second crystals; these profiles represent the reflectivity of the crystals as a function of the glancing angle for strictly monochromatic incident radiation. These functions are given by the Darwin–Prins theory, and the present calculations were performed with an algebraic reduction of this theory which was developed by Miller (1935). In this formulation the Darwin–Prins functions are given by

$$I(l) = G(l) - [G^2(l) - 1]^{\frac{1}{2}} , \quad (2a)$$

where

$$G(l) = \frac{\delta^2}{A^2 + B^2} \left\{ l^2 + \frac{\beta^2}{\delta^2} \right.$$
$$\left. + \left[(l^2 - \alpha^2)^2 + \frac{4\beta^2}{\delta^2} (l + \frac{AB}{\delta\beta})^2 \right]^{\frac{1}{2}} \right\} , \quad (2b)$$

$$\alpha^2 = (A^2 - B^2 + \beta^2)/\delta^2 , \quad (2c)$$

$$l = (\theta - \theta_0)(\sin 2\theta_0/2\delta) - 1 , \quad (2d)$$

$$A + iB = \mathscr{P}e^{-w} \left(\frac{N\lambda^2}{2\pi} \right) \left(\frac{e^2}{mc^2} \right) F . \quad (2e)$$

In these equations θ' and θ_0 have the same meaning as in equation (1); N represents number of unit cells per unit volume, F is the crystal structure factor *for the particular reflecting plane employed*; δ and β are the real and imaginary parts of the complex index of refraction of the crystal for the wavelength λ, e^2/mc^2 is the classical electron radius, e^{-w} is the single crystal Debye–Waller factor, and $\mathscr{P}$ is the polarization factor ($\mathscr{P} = 1$ for σ polarization and $\mathscr{P} = |\cos 2\theta|$ for π polarization).

If the double-crystal reflection is normalized to the intensity reflected from the first crystal, and account is taken of both polarizations, equation (1) may be rewritten as

$$P(\psi) = \frac{\int_{-\phi_m}^{\phi_m} G(\varphi) S(\psi - \varphi^2 \tan \theta_0) d\varphi}{\int_{1-\phi_m}^{\phi_m} G(\varphi) d\varphi} , \quad (3a)$$

where

$$S(\psi - \varphi^2 \tan \theta_0) = \frac{\int_{-\infty}^{\infty} [I_1^\sigma(\tilde{\theta}) I_2^\sigma(\psi - \varphi^2 \tan \theta_0 - \tilde{\theta}) + I_1^\pi(\tilde{\theta}) I_2^\pi(\psi - \varphi^2 \tan \theta_0 - \tilde{\theta})] d\tilde{\theta}}{\int_{-\infty}^{\infty} [I_1^\sigma(\tilde{\theta}) + I_1^\pi(\tilde{\theta})] d\tilde{\theta}} , \quad (3b)$$

and $\tilde{\theta} = \theta - \theta_0 - (\varphi^2/2)\tan\theta_0$; the dependence of $G(\theta, \varphi)$ on θ is assumed negligible in the range for which $I(\theta)$ is appreciable.

For the present experiment, the effects of vertical divergence on equation (3a) were evaluated using the procedure developed by Shacklett & DuMond (1937). Their treatment assumed equal slit heights and required S to be Lorentzian; in an unpublished calculation one of the authors (J.S.T.) has eliminated the latter requirement by leaving S general and expanding it in a Taylor series. His treatment employs a parameter $k = (\varphi_m^2 \tan\theta_0)/w_S$, where w_S is the half-intensity width of S (in radians); the difference between $P(\psi)$ and $S(\psi)$ is expressed as a power series in k, provided $k < 1$. The first order term in the series merely translates the ψ axis by $(\varphi_m^2 \tan\theta_0)/12$, but leaves the shape of the two curves the same. The second order term produces primarily a broadening of $P(\psi)$; for the Lorentzian case the width becomes $w_P = w_S(1 + 0.06k^2)$.

The first order shift is in agreement with the vertical divergence correction obtained by Williams (1932), $\Delta\theta = (\tan\theta_0)(a^2 + b^2)/24L^2$, where a and b are the respective heights of two slits that are separated by a distance L. For equal slit heights with $a = b$ this reduces to the Thomsen result. In the present experiment $\varphi_m < 4 \times 10^{-3}$ radians, and $k^2 < 0.1$, and the vertical divergence effects on the shape of the monochromatic profiles were found to be within the experimental errors and hence were neglected. The data were compared directly with $S(\psi)$.

The evaluation of $S(\psi)$ required numerical integration, and it was found convenient to rewrite equation (3b) as the sum of three terms (concentrating for the moment on a single polarization component),

$$S(\psi) = (1/\mathrm{NF})\,[S_1(\psi) + S_2(\psi) + S_3(\psi)\,], \qquad (4a)$$

$$S_1(\psi) = \int_{\theta^*}^{\infty} I_1(\psi/2 - \theta')I_2(\psi/2 + \theta')d\theta', \qquad (4b)$$

$$S_2(\psi) = \int_{-\theta^*+\psi/2}^{\theta^*+\psi/2} I_1(\tilde{\theta})I_2(\psi - \tilde{\theta})d\tilde{\theta}, \qquad (4c)$$

$$S_3(\psi) = \int_{\theta^*}^{\infty} I_1(\psi/2 + \theta'')I_2(\psi/2 - \theta'')d\theta'', \qquad (4d)$$

$$\mathrm{NF} = \int_{-\theta^*}^{\theta^*} I_1(\tilde{\theta})d\tilde{\theta} + \mathrm{ENF}, \qquad (4e)$$

$$\mathrm{ENF} = \int_{-\infty}^{-\theta^*} I_1(\tilde{\theta})d\tilde{\theta} + \int_{\theta^*}^{\infty} I_1(\tilde{\theta})d\tilde{\theta}. \qquad (4f)$$

In these equations, $\theta' = \psi/2 - \tilde{\theta}, \theta'' = -\theta'$, and for the usual case of the same reflection from identical first and second crystals, $I_1(\tilde{\theta}) = I_2(\tilde{\theta})$ and $S_1 = S_3 = S^*$.

For reasonably chosen values of θ^*, S^* was shown to produce negligible contributions to S, and hence could be ignored. This fact was established by using the no-absorption Darwin functions I_1^D and I_2^D in place of the Darwin–Prins functions I_1 and I_2, and integrating analytically to obtain an upper limit for S^*. For this calculation, I_1^D and I_2^D were obtained from equations (2) as the limit when B and β approach zero. With the use of appropriate Taylor series expansions it was then possible to obtain an estimate for $S^*(\psi)$. This quantity is also a function of θ^*, which may be re-expressed as l^* through equation (2d).

With $l^* = 3$ and $-2 \leq \psi \leq 2$, it was found that $S^* < 10^{-3}S_2$, i.e. that S^* is less than 0.1% of the contribution to S in the peak region. The demonstration of this property for the normalizing factor NF proceeded along the same lines, but in this case the contribution of ENF (for $l^* = 3$) represented about 5% of the total value of NF. ENF had therefore to be calculated analytically and added to the result of the numerical integration of the peak region.

The numerical integration of S_2 and NF was computed by Simpson's rule on an IBM 7094 computer. The crystal planes studied were quartz ($10\bar{1}1$), silicon (111), calcite (211) ($10\bar{1}4$), and germanium (111), where the indices refer to the structural cells; the necessary input data for the computer calculations are given in Table 1. The resulting values of $P(\psi)$ are plotted as solid curves in Figs. 2–5.

Experimental details

These theoretical curves were checked against the data obtained from the experimental set-up shown in Fig. 1. The Mössbauer source was prepared by plating 170 millicuries of ^{57}Co onto two pieces of ^{56}Fe (99.9% enriched) foil of dimensions $10 \times 5 \times 0.005$ mm. The foils were annealed and each was sealed into a 0.005 mm thick aluminum envelope to prevent oxidation. The envelopes were mounted one on top of the other, and the whole assembly was given a horizontal inclination with respect to the direction of the γ beam so as to foreshorten the source dimensions to a vertical line 10 mm high with a projected width of 2 mm.

The vertical divergence of the γ beam was limited to $\pm 12'$ of arc about the horizontal by a Soller slit system (Soller, 1924), which was used in conjunction with the other defining slits and lead shielding to re-

Table 1. *Parameters required for the calculation of Darwin–Prins functions*

	δ	β	A	B	e^{-w}
Quartz ($10\bar{1}1$)	2.66×10^{-6}	1.14×10^{-8}	7.37×10^{-7}	5.22×10^{-9}	0.98
Silicon (111)	2.37×10^{-6}	1.77×10^{-8}	1.24×10^{-6}	1.25×10^{-8}	0.99
Calcite (211) ($10\bar{1}4$)	2.72×10^{-6}	2.51×10^{-8}	1.33×10^{-6}	2.39×10^{-8}	0.96
Germanium (111)	4.7×10^{-6}	4×10^{-7}	2.8×10^{-6}	2.8×10^{-7}	0.99

duce the total solid angle for emission of radiation from the source to 10^{-4} steradians. The double crystal spectrometer was of the conventional slide design (Sandström, 1957), and the angle of rotation of the second crystal was measured interferometrically (Marzolf, 1964) with an accuracy of $\pm 0.05''$. A $12 \times 6 \times 0.4$ mm NaI (Tl) crystal mounted on an EMI 6097B photomultiplier was used as the γ detector, and this was heavily shielded to obtain a low background (about one count per minute).

The crystals were prepared by grinding the reflecting surfaces parallel to the atomic planes (within $20''$ of arc) and etching until the minus position widths with Mo $K\alpha$ X-rays reached a minimum. To obtain the diffraction profiles, several runs were made with each crystal pair. The count rate (0.2–0.4 count.sec^{-1}) was extremely low compared with a conventional X-ray source. Approximately 100 counts were recorded at each spectrometer setting (about every half second of arc). The counts at the respective points were then added to give the final profile, resulting in a statistical error (standard deviation) of about 3% for most of the data points. Atmospheric pressure and room temperature changes were monitored, and possible errors in the angle-measuring interferometer and crystal lattice due to these effects were checked and found to be negligible.

Since the ^{57}Co $\rightarrow$ ^{57}Fe decay gives rise to a 122 keV γ as well as the 14·4 keV Mössbauer photon (also, of course, a 6·3 keV internal conversion Fe $K\alpha$ X-ray), it was necessary to check that all γ intensities measured were due to the desired 14·4 keV photons. Therefore, additional measurements were made on the direct and reflected beams with brass and aluminum absorbers placed immediately in front of the source. The direct beam contained an appreciable fraction of 122 keV γ rays, and a small fraction of these were Compton scattered into the beam reflected from the first crystal. On the other hand, after reflection from the second crystal, the beam was found to contain only the 14·4 keV photons.

Corrections have been applied for the ordinary background, which was determined with the set-up arranged exactly as for a double-crystal measurement, but with a small lead plate blocking the beam between the first and second crystals. Background was also determined without the lead stop but with the second crystal turned about 2° away from the Bragg angle, and both determinations produced the same result. Since the beam intensity reflected from either the first or second crystals was so low, there was no dead time correction.

Discussion of results

The experimental data are compared with theory in Figs. 2–5. The errors displayed there are standard deviations, and the count rate scale has been selected to match the theory at the peak. The origin for the angle coordinate (plotted as the abscissa) has been chosen to provide the best fit, since it is impossible to determine this origin unambiguously without independent knowledge of both the γ-ray wavelength and the crystal lattice constant. Such knowledge, however, does not exist independently of this type of measurement. Thus the figures compare only the *shapes* of the observed profiles with those of the calculated ones.

Comparison of theory and experiment for both tails, far to the right and left of the plotted portion, is shown in Table 2. In general, the experimental values are several times as large as the theoretical ones.

Table 2. *Comparison of experimentally measured reflected fractions with computed values (Darwin–Prins theory) in tails of profiles*

Crystal	Displacement from peak (sec)	Experimental fraction	Computed fraction
Quartz (10$\bar{1}$1)	−8·9	0·030 ± 0·003	0·008$_3$
(Fig. 2)	+8·8	0·031 ± 0·003	0·008$_5$
Silicon (111)	−8·5	0·133 ± 0·005	0·019
(Fig. 3)	+8·6	0·132 ± 0·007	0·019
Calcite (211)	−11·5	0·053 ± 0·003	0·013
(10$\bar{1}$4) (Fig. 4)	+10·9	0·063 ± 0·003	0·015
Germanium (111)	−18·8	0·035 ± 0·002	0·016
(Fig. 5)	+16·3	0·046 ± 0·003	0·021

The general agreement with the theory is good. In the case of quartz (Fig. 2) the single-crystal pattern is relatively flat-topped and the data show clearly the
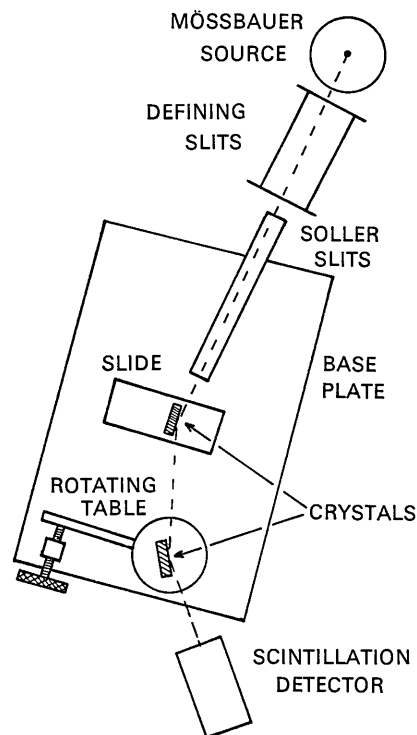

Fig. 1. Schematic diagram of experimental arrangement. The defining slits were separated by 30 cm and the Soller slit system was 43 cm in length.

symmetric, straight-edged, sharp-peaked double crystal profile which is characteristic of the convolution of two such flat-topped functions. This quartz run establishes the symmetry clearly, and indicates the suitability of quartz (at least this particular pair of crystals) for spectroscopic use.

The silicon data (Fig. 3) give a second example of the symmetric single-crystal pattern. In this case, the wider silicon profile (the second crystal) is scanned with a narrower quartz pattern (the first crystal) and the resulting function is qualitatively quite similar to the flat-topped single crystal profile of silicon. This flat top in the two-crystal pattern occurs where the flat region of the quartz is probing entirely within the flat region of the silicon profile.

On either side of this flat region, however, the experimental curve slopes down considerably more slowly than the theory predicts. This is a common occurrence
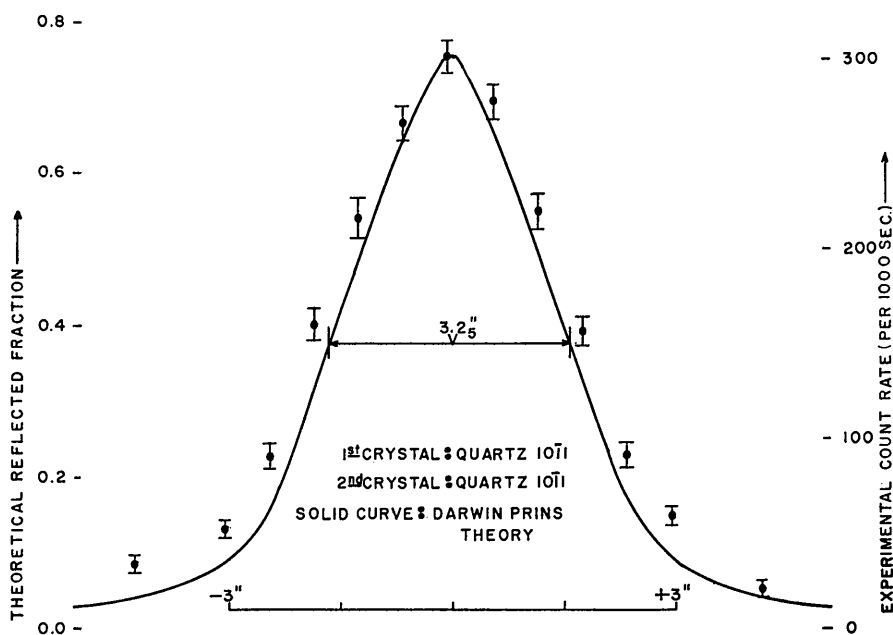

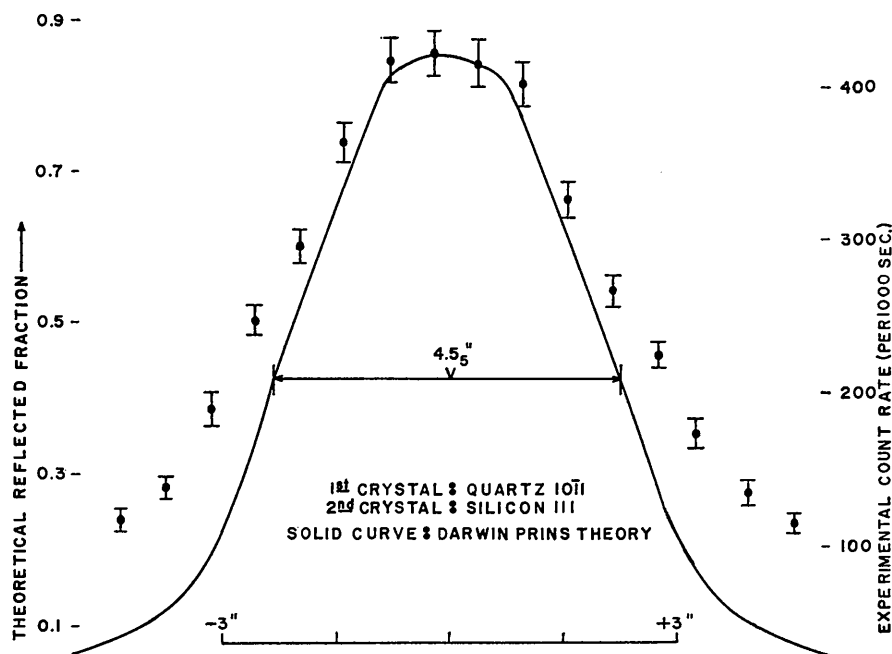Fig. 2. Theoretical and experimental double-crystal monochromatic profiles for quartz (10$\bar{1}$1).

Fig. 3. Theoretical and experimental double-crystal monochromatic profiles for silicon (111) (with quartz (10$\bar{1}$1) as first crystal).

in crystal studies (Renninger, 1955, 1960) and may be produced at will by merely grinding the front face of the crystals. In fact, the theory shows that any imperfections such as dislocations or mosaic block structure (disorientation of small segments of the crystal face against the main structure of the lattice) produce broader and less steep peaks. Although etching the crystal eliminates the mosaic structure produced in grinding, there is no way to correct a high dislocation

density throughout the entire volume of the crystal. The calcite data shown in Fig. 4 are subject to the same considerations.

Germanium shows the other extreme – a pronounced asymmetry. This is unambiguously indicated by the experimental data shown in Fig. 5, where the general shape, overall width, and relative height of the tails are in reasonable agreement with the theory. It is clear that this asymmetry would produce a significant error
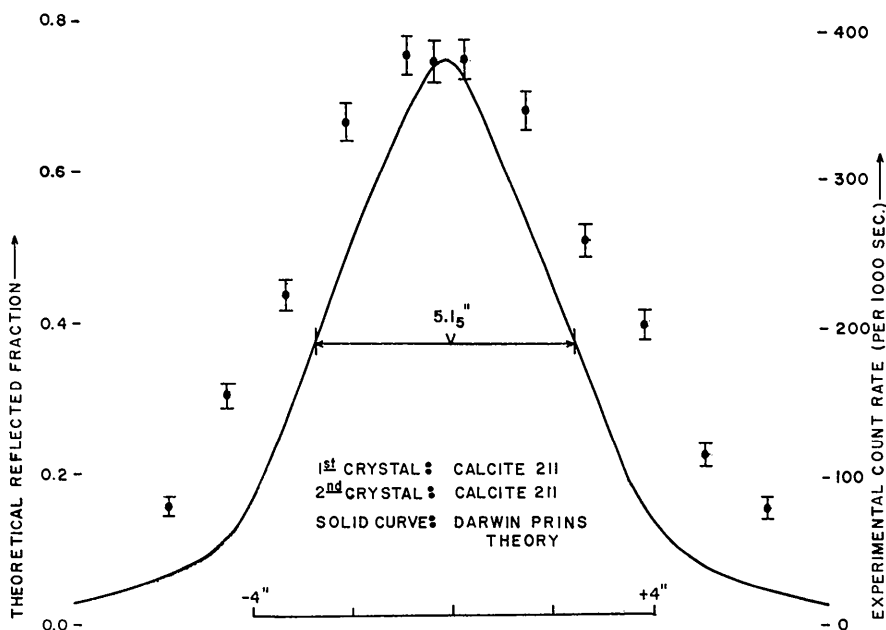
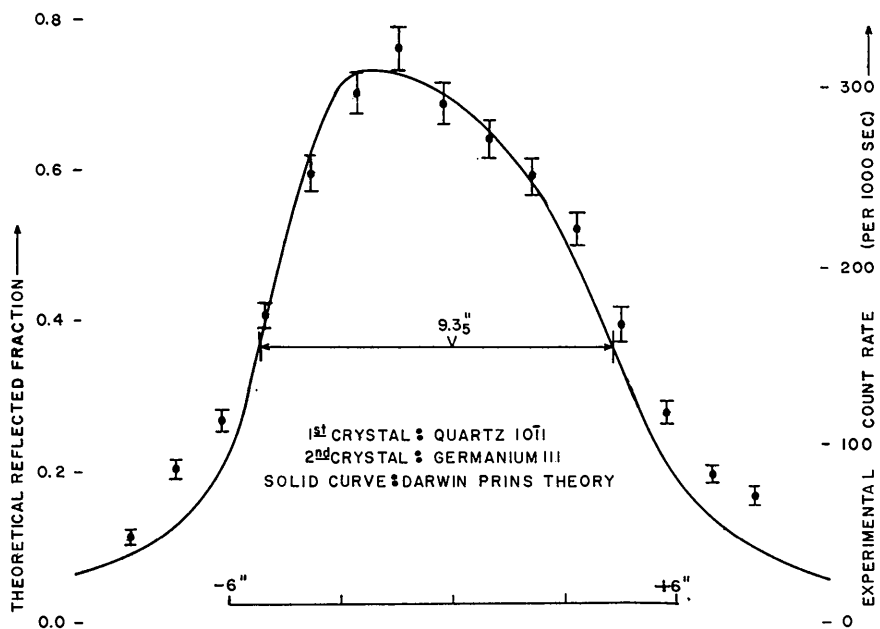Fig. 4. Theoretical and experimental double-crystal monochromatic profiles for calcite (211) (10$\bar{1}$4).

Fig. 5. Theoretical and experimental double-crystal monochromatic profiles for germanium (111) (with quartz (10$\bar{1}$1) as first crystal).

if such crystals were used in precision spectroscopy. The Darwin–Prins theory, however, may be used to correct for this asymmetry in the instrumental window. The magnitude of the calculated correction (at $\lambda =$ 0·86 Å*) is such that the wavelength of monochromatic radiation as measured by a pair of Ge (111) crystals would be less than the true value by 17 ppm. The correction is approximately the same whether the peak or the average of the two half-intensity points is chosen as the wavelength criterion. In ordinary X-ray spectroscopy, the width of a spectral line is considerably greater than the width of the instrumental window, and in this case the appropriate corrections may be obtained from the Darwin–Prins theory by a method developed by Sauder (1966).

References

ALLISON, S. K. (1932). Phys. Rev. 41, 1.
BORRMANN, G. (1941). Physik. Z. 42, 157.
BORRMANN, G. (1950). Z. Physik. 127, 297.
BROGREN, G. & ADELL, O. (1954). Ark. Fysik 8, 97, 401.
BOLLMANN, V. L., BAILEY, H. H. & DuMOND, J. W. M. (1938). Phys. Rev. 54, 792.
BUBÁKOVÁ, R., DRAHOKOUPIL, J. & FINGERLAND, A. (1960). Czech. J. Phys. B10, 255.
BUBÁKOVÁ, R., DRAHOKOUPIL, J. & FINGERLAND, A. (1961). Czech. J. Phys. B11, 199.
COMPTON, A. H. & ALLISON, S. K. (1935). X-Rays in Theory and Experiment, 2nd ed. p. 709 ff. New York: Van Nostrand.
DARWIN, C. G. (1914). Phil. Mag. 27, 315, 675.
DuMOND, J. W. M. (1937). Phys. Rev. 52, 872.
KOHRA, K. (1962). J. Phys. Soc. Japan, 17, 589.
MARZOLF, J. G. (1964). Rev. Sci. Instrum. 35, 1212.
MILLER, F. JR (1935). Phys. Rev. 47, 209.
PARRATT, L. G. (1932). Phys. Rev. 41, 561.
PARRATT, L. G. & MILLER, F. JR (1936). Phys. Rev. 49, 280.
PRINS, J. A. (1930). Z. Physik, 63, 477.
RENNINGER, M. (1955). Acta Cryst. 8, 597.
RENNINGER, M. (1960). Acta Cryst. 13, 1067.
RENNINGER, M. (1967). Advanc. X-Ray Analysis, 10, 32.
SANDSTRÖM, A. E. (1957). Handbuch der Physik, 30, 106, edited by S. FLÜGGE. Berlin: Springer-Verlag.
SAUDER, W. C. (1966). J. Appl. Phys. 37, 1495.
SCHWARZSCHILD, M. (1928). Phys. Rev. 32, 162. (In the expression for R following equation (19) of this paper there is a sign error in the δ_2 term.)
SHACKLETT, R. L. & DuMOND, J. W. M. (1957). Phys. Rev. 106, 501.
SOLLER, W. (1924). Phys. Rev. 24, 158.
WILLIAMS, J. W. (1932). Phys. Rev. 40, 636.

Symmetry in the Generation of Trial Structures

BY F. L. HIRSHFELD*

University Chemical Laboratory, Lensfield Road, Cambridge, England

In the generation of trial structures by the systematic variation of the position and orientation of a molecule of known dimensions, the ranges to be scanned by the positional and orientational parameters depend on the symmetry of the molecule and on the space group. The set of transformations of the crystal axes that leave invariant the coordinates of equivalent positions for a given space group defines a corresponding derivative symmetry, conforming to one of thirty distinct 'Cheshire' groups. The direct product of this group with the molecular point group specifies the symmetry of the six-dimensional space of the trial-structure parameters. The asymmetric unit in this space is the region to be scanned by the several parameters.

Trial-structure parameters defined

A recurring problem is the determination of the structure of a crystal whose asymmetric unit comprises a chemical entity, e.g. a molecule, of known or reasonably conjectured internal dimensions. The initial task, estimating the position and orientation of the molecule in the unit cell, may often be amenable to some kind of trial-and-error approach. Whatever the criterion chosen for judging the acceptability of a trial structure, some systematic procedure is needed for generating alternative models compatible with the available structural information. We suppose here that this information comprises the cell dimensions, the space group, and the postulated molecular dimensions. Our formu-

---

* On leave from Department of Chemistry, Weizmann Institute of Science, Rehovoth, Israel.